

Numerical Simulation of Unsteady Viscous Flow Around a Flapping Wing

Koji Isogai

Department of Aeronautics and Astronautics

Kyushu University

6-10-1 Hakozaki, Higashiku, Fukuoka 812-8581, Japan

E-mail: isogai@aero.kyushu-u.ac.jp

Key words: flapping wing, dynamic stall

Abstract. In order to investigate the effects of dynamic stall phenomenon on the propulsive efficiency, thrust and lift of flapping wing of a bird, unsteady viscous flow simulations have been performed by using a 3D Navier-Stokes code. As a result of the simulations about a typical pigeon wing which has thick-large-cambered airfoil sections and a peculiar nose-up twist distribution, it is shown that the occurrence of the flow separation is unavoidable around the tip region to maintain the high lift and appropriate thrust, wherefore the propulsive efficiency remains less than 0.5. This is in sharp contrast with the results of the existing potential flow analyses that predict the very high propulsive efficiency of the order of 0.8~0.9.

1 Introduction

Unlike aircraft, a bird should generate lift and thrust at the same time by a flapping motion of a wing. In order to investigate the aerodynamic mechanism of generating lift and thrust by a flapping wing, many theoretical¹⁾⁻²⁾ and experimental studies³⁾⁻⁴⁾ have been conducted so far. However, the mechanism has not yet been well understood. As far as the three-dimensional (3D) wing is concerned, all the theoretical studies presented so far are based on the potential flow assumption. As you can see in the flying birds, however, the amplitude of the flapping motion of the wing is very large (for example, the flapping angle of a pigeon is about 50 deg as shown later in the example). In such a large amplitude of the flapping motion, the induced angle of attack (due to the flapping motion of a wing) exceeds easily stalling angle. This means that the discussions based on the potential flow assumption become meaningless. In the present study, the numerical simulation of unsteady viscous flow around a flapping wing has been conducted by using a 3D Navier-Stokes code and the role of the flow separation, especially, the effect of dynamic stall on the propulsive efficiency, thrust and lift of a flapping wing has been investigated.

2 Method of Analysis

As is well known, the basic motion of a bird wing is a coupled oscillation of flapping and feathering (twisting motion). As defined in Fig. 1, the vertical displacement of the arbitrary point of the upper/lower surfaces of the wing can be expressed as

$$y(x, z, t) = y_s(x, z) + f(x, z, t) \quad (1)$$

where y_s is the time-mean displacement of the upper/lower surfaces, and where f is

the displacement of the upper/lower surfaces from the time-mean displacement y_s . $f(x,z,t)$ in Eq. (1) can be given by

$$f(x,z,t) = (h_r + \phi_0 z) \sin(kt) - (\theta_r + b_\theta z)(x - x_p(z)) \sin(kt + \phi) \quad (2)$$

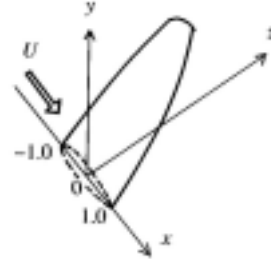


Fig. 1 Definitions of coordinate and wing motion.

where k is the reduced frequency based on the root semichord b_r and is defined by $k=(b_r\omega)/U$, where ω is the circular frequency of the wing and U is the free-stream velocity. In Eqs. (1) and (2), all the physical quantities are nondimensionalized by b_r . In Eq. (2), t is the dimensionless time, and h_r is the amplitude of the heaving oscillation at the root station, and ϕ_0 is the amplitude of the flapping oscillation, and θ_r is the amplitude of the pitching oscillation at the root station. The amplitude of the pitching oscillation is assumed to increase linearly toward tip station with the slope of b_θ , and x_p is the x coordinate of the pitch axis, and ϕ is the phase-advance angle of the pitching oscillation ahead of the flapping oscillation. In order to compute the unsteady viscous flow around the oscillating wing whose motion is given by Eq. (1), a 3D compressible Navier-Stokes code is applied. The grid used is C-H type structured grid, 240(chord wise)x31(normal to surfaces)x19(span wise). In the computations, Mach number and Reynolds number are assumed to be 0.30 and 10^5 , respectively, and Baldwin & Lomax's algebraic turbulence model⁵⁾ is employed.

3 Results and Discussion

3-1 Code Validation

Since, as far as we concern a 3D flapping wing, there is no existing NS computation nor reliable experimental data that are published so far, we will compare our NS computations with those of the 3D potential theories. The case we have selected is a rectangular wing of aspect ratio 8 oscillating in a coupled heaving and pitching, for which the potential flow computation by Lan²⁾, who employed Unsteady Quasi-Vortex Lattice Method (UQVLM), exists. The details of the wing motion are as follows: $k=0.25$, $h_r=2.0$, $\phi_0=0$ deg, $\theta_r=23$ deg, $x_p=0.5$. The wing section is NACA0012 and the mean angle of attack is 0 deg. The results of the present NS simulation for this case are as follows: propulsive efficiency $\eta_p=0.70$ ($\eta_p = TU/W$, T : time mean thrust, W : time mean rate of work), thrust coefficient $C_T=0.0623$ ($C_T=T/(1/2\rho U^2S)$). The results obtained by Lan²⁾ for this case by using UQVLM are $\eta_p=0.94$ and $C_T=0.0623$. Since no viscous effect is included in those obtained by Lan, those of our present NS simulation seem to be reasonable.

3-2 Numerical Example and Discussion

In the following examples, we will show that the occurrence of flow separation reduces the propulsive efficiency and thrust considerably. The wing studied is a straight tapered wing of aspect ratio 7.04 and the taper ratio 0.42. The wing section is NACA0012 and the mean angle of attack is assumed to be 0 deg. b_r and U are assumed to be 0.0905m and 11m/s, respectively. For this wing, we have computed two cases of different oscillation mode. The reduced frequency k is 0.30. The first case is for a pure flapping motion ($\phi_0=33$ deg) without twist. In Fig. 2, the flow pattern (iso-vorticity distribution) at $kt=\pi$ where the maximum effective angle of attack induced by the flapping motion becomes 31 deg at 75% semispan station is

shown. As seen in the figure, the large scale flow separation can be seen from 50% semispan station to the tip station. η_p and C_T for this case are 0.111 and 0.0374, respectively. The second case is for a coupled flapping and feathering motion, namely, $\phi_0=33$ deg, $\theta_r=0$ deg, $b_0=0.0931$ (the pitch amplitude at 75% semispan station is about 20 deg). In this case, the maximum effective angle of attack at 75% semispan station is about 11 deg. The flow pattern at $kt=\pi$ where the effective angle attack becomes maximum is shown in Fig. 3. As seen in the figure, there is no large scale flow separation. η_p and C_T for this case are 0.619 and 0.106, that are considerably higher than those of the first case. In Fig. 4, the variations of thrust and rate of work for the two cases are shown. As seen in the figure, the second case (the coupled flapping and feathering motion) generates considerably higher thrust by consuming a smaller amount of energy compared with the first case (the pure flapping motion without twist).

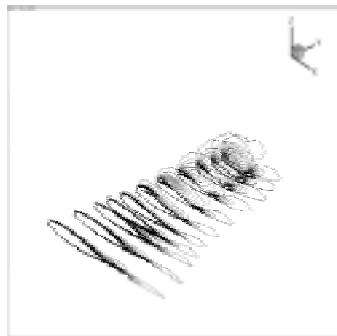


Fig. 2 Flow pattern at $kt=\pi$ (pure flapping).

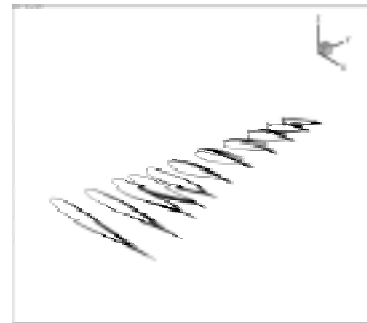


Fig.3 Flow pattern at $kt=\pi$ (coupled flapping and pitching).

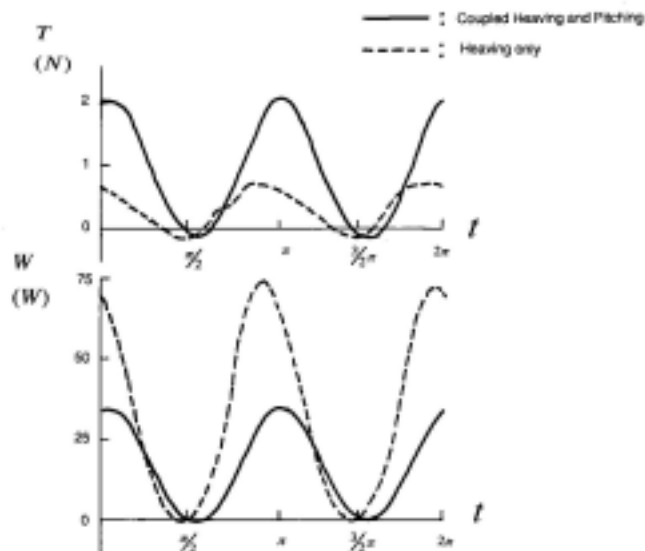


Fig. 4 Variations of thrust and rate of work.

As an example of more realistic case where thrust and lift are generated at the same time, the flow around a pigeon wing shown in Fig. 5 is computed. In Fig. 5, the plan form, wing section and the geometrical twist distribution, that are measured by Nachtigall and Wieser⁶⁾, are shown. The detailed values of the wing geometry are as follows: the aspect ratio is 7.2, full span length is 0.66 m, $br=0.055$ m, full span wing area is 0.062 m², mass is 0.39 Kg. As to the wing motion, the following values at the cruise condition ²⁾ are taken, that is, $U=11$ m/s, $\omega=50.24$ rad/s, $k=0.25$, $h_r=0.0$, $\phi_0=50$ deg, $\theta_r=0$, $b_0=0.129$ (pitching amplitude is 30.4 deg at 75% semi-span station), $\phi=90$ deg, $x_p=-0.50$.

The results of the numerical simulation for this case are as follows: propulsive efficiency $\eta_p=0.42$, thrust coefficient $C_T=0.12$, lift coefficient $C_L=0.72$. Vest and Katz²⁾ have computed the same case by using a panel method, obtaining $\eta_p =0.64$, $C_T=0.13$, $C_L=0.85$. In our computations, the large scale flow separation is observed, as shown in Fig. 6 (iso-vorticity in z direction contour), on the upper surface from 70% semispan to tip station at the instant of $kt=\pi$ when the induced angle of attack becomes maximum. Since the occurrence of the flow separation reduces the propulsive efficiency considerably⁷⁾, the results we have obtained seem to be quite reasonable compared with those obtained by Vest and Katz²⁾ by using the panel method. In Fig. 7, the variations of lift, thrust and rate of work during one cycle of oscillation are shown. In the figure, it can be seen that most of the lift and thrust are generated during the process of down stroke ($kt=\pi/2 - 3/2\pi$).

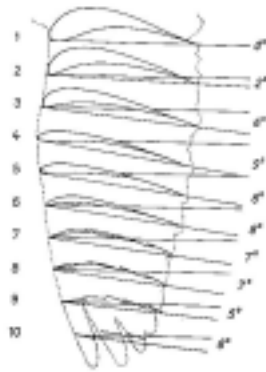


Fig. 5 Planform and wing sections of a pigeon wing (Nachtigall and Wieser⁶⁾).

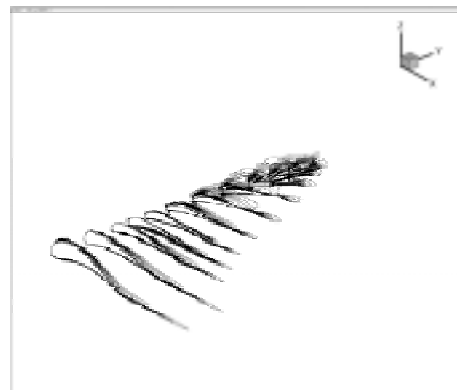


Fig. 6 Flow pattern at $kt=\pi$.

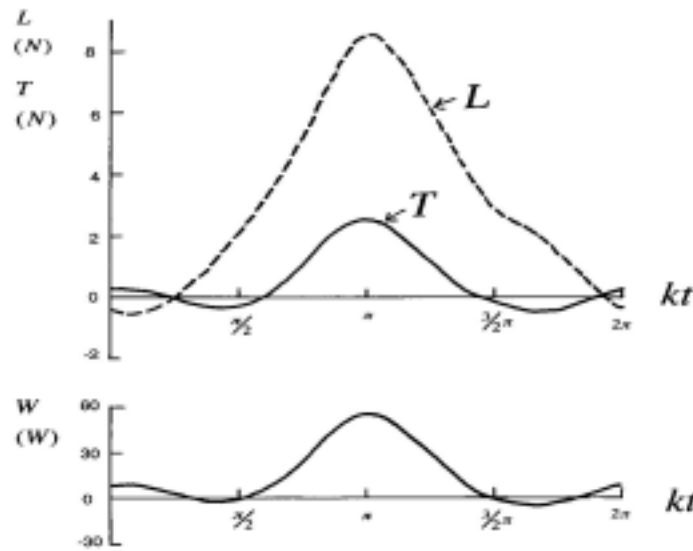


Fig. 7 Variations of lift, thrust and rate of work during one cycle of oscillation.

By the present numerical simulations of the unsteady viscous flow around the pigeon wing, it is disclosed that the requirements of obtaining high lift and high propulsive efficiency at the same time are contradictory. That is, in order to obtain the high mean lift such as the present pigeon case (C_L required to sustain its weight at $U=11$ m/s is 0.83), the maximum effective angle of attack in the process of down stroke, which is induced by the flapping motion, easily exceeds the stalling angle, and that results in considerable reduction of the propulsive efficiency. It is conjectured, however, that the large cambered airfoil sections and the peculiar built-in twist distribution of the present pigeon wing seem to be the device to attain these contradictory requirements as high as possible.

4 Conclusion

Numerical simulations of unsteady viscous flow around a flapping wing have been conducted by using a 3D Navier-Stokes code, and the following results have been obtained. 1) The occurrence of flow separation reduces the propulsive efficiency and thrust considerably. 2) The propulsive efficiency and thrust can be improved considerably by adding the appropriate twisting motion to the flapping motion, that prevents the flow separation. 3) The numerical simulation of a flapping pigeon wing which has large cambered airfoil sections and a peculiar built-in twist distribution has revealed that the flow separation is unavoidable around the tip region to maintain the high lift and appropriate thrust, wherefore the propulsive efficiency remains less than 0.5. 4) Although requirements of obtaining high lift and high propulsive efficiency at the same time are contradictory, the large cambered airfoil sections and the peculiar built-in twist distribution of the pigeon wing seem to be the device to attain these contradictory requirements as high as possible.

References

1. Lan, C.E.,J.: Fluid Mechanics, Vol. 93, Part 4, pp. 747-765 (1979).
2. Vest, M.S. and Katz, J.: AIAA Journal, Vol. 34, No.7, pp. 1435-1440 (1996).
3. Fejtek, I. And Nehera, J.: Aeronautical Journal, Vol. 84, pp. 28-33 (1980).
4. Vest, M.S. and Katz, J. : AIAA 99-0994, Jan. (1999).
5. Baldwin, B.S. and Lomax, H., AIAA Paper 78-257, (1978).
6. Nachtigall, W. und Wieser, J.: Zeitschrift fur vergleichende Physiologie 52, pp. 333-346 (1966).
7. Isogai, K., Shinmoto, Y. and Watanbe, Y.: AIAA Journal, Vol. 37, No. 10, pp. 1145-1151 (1999).